Adaptation in a revised inner-hair cell model

Christian J. Sumner[a)]
Centre for the Neural Basis of Hearing at Essex, Department of Psychology, University of Essex, Colchester CO4 3SQ, United Kingdom

Enrique A. Lopez-Poveda
Centro Regional de Investigación Biomédica, Facultad de Medicina, Universidad de Castilla—La Mancha, Campus Universitario, 02071 Albacete, Spain

Lowel P. O'Mard and Ray Meddis
Centre for the Neural Basis of Hearing at Essex, Department of Psychology, University of Essex, Colchester CO4 3SQ, United Kingdom

(Received 29 March 2002; revised 24 August 2002; accepted 30 August 2002)

A revised computational model of the inner-hair cell (IHC) and auditory-nerve (AN) complex was recently presented [Sumner *et al.*, J. Acoust. Soc. Am. **111**, 2178–2188 (2002)]. One key improvement is that the model reproduces the rate-intensity functions of low- (LSR), medium- (MSR), and high-spontaneous rate (HSR) fibers in the guinea-pig. Here we describe the adaptation characteristics of the model, and how they vary with model fiber type. Adaptation of the revised model for a HSR fiber is in line with an earlier version of the model [Meddis and Hewitt, J. Acoust. Soc. Am. **90**, 904–917 (1991)]. In guinea-pig, poststimulus time histograms (PSTH) have been found to show less adaptation in LSR fibers. Evidence from chinchilla suggests that this is due to chronic adaptation resulting from short interstimulus intervals, and that fully recovered LSR fibers actually show more adaptation. However, the model is able to account for both variations of PSTH shape when fully recovered from adaptation. Interstimulus interval can also affect recovery in the model. The model is further tested against data previously used to evaluate models of AN adaptation. The tests are (i) recovery from adaptation of spontaneous rate and (ii) the recovery of response to acoustic stimuli (''forward masking''), (iii) the response to stimulus increments and (iv) decrements, and (v) the conservation of transient components. A HSR model fiber performs similarly to the earlier version of the model. However, there is considerable variation in response to increments and decrements between different model fibers.
[DOI: 10.1121/1.1515777]

PACS numbers: 43.64.Bt, 43.66.Ba [LHC]

I. INTRODUCTION

We have recently presented a revised version (Sumner *et al.*, 2002) of an earlier inner-hair cell (IHC) auditory-nerve (AN) model (Meddis, 1986, 1988; Meddis *et al.*, 1990). This model combines a modified bio-physical model of the receptor potential, a calcium-driven mechanism for neurotransmitter release, and a quantal-stochastic version of the Meddis IHC model of transmitter recycling. The model is able to reproduce the rate-intensity functions of low- (LSR), medium- (MSR), and high-spontaneous rate (HSR) fibers, when used with a suitable nonlinear model of cochlear mechanical filtering. The fiber type is largely determined by the number of calcium channels near the synapse. A striking feature of AN activity is the reliable reduction in firing rate during the response to a stimulus of more than a few milliseconds. This characteristic has been a topic of detailed study in the past (e.g., Smith, 1977; Westerman, 1985; Yates *et al.*, 1985). The original IHC model (Meddis, 1986, 1988) was conceived in large part to account for the adaptation of firing rate observed in the AN. Like other models proposed at the time (e.g., Westerman and Smith, 1988), it modeled the average characteristics of AN adaptation. Since the majority of fibers are of the HSR type, the models are representative of these. However, differences in adaptation have been reported for different fiber types. Here we report on the adaptation characteristics of the new model, and how these adaptation characteristics depend on the fiber type being modeled.

In the first part of this study we attempt to reproduce the reported differences in poststimulus time histogram (PSTH) with fiber type. In the second part, we test six model fibers against data that have been previously used to test models of AN adaptation, in order to facilitate comparisons. Third, we examine the inner workings of the model.

II. THE MODEL

The IHC model is employed as part of a complete peripheral model. This consists of four components: bandpass filtering by the middle-ear; nonlinear mechanical filtering by the cochlea; and IHC transduction and refractory effects of the AN. These components are described fully by Sumner *et al.* (2002).

The IHC model consists of three stages. The output from

[a)]Author to whom correspondence should be addressed. Kresge Hearing Research Institute, University of Michigan, Ann Arbor, MI 48109-0506. Electronic mail: cjsumner@umich.edu

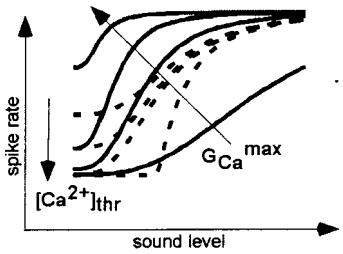

FIG. 1. Effect of varying calcium transmitter release mechanism parameters, G_{Ca}^{max} and $[Ca^{2+}]_{thr}$, on rate-intensity functions. Arrows show the direction of function change for an increase in each parameter value.

the mechanical filtering stage drives a biophysical model of the IHC, modified from a model proposed by Shamma *et al.* (1986). This reproduces realistic receptor potentials (RPs). The RP drives a simple model of the calcium ion movement in the vicinity of the synapse. The local calcium concentration determines the release probability of any neurotransmitter that is available for release. The neurotransmitter cycles around the synapse according to the scheme proposed by Meddis (1986, 1988), except that the transmitter is now contained in discrete packets within the hair-cell. These vesicles are released stochastically into the synaptic cleft, where they can cause the postsynaptic AN to fire. If the AN is not in a refractory state, a single quantum of transmitter released into the cleft will produce an action potential. The rate limited cycling of the neurotransmitter reproduces the adaptation observed in the AN.

In this study we are concerned with the calcium-based transmitter release function, and the movement of neurotransmitter around the synapse. The inward calcium current (I_{Ca}) in the vicinity of a hair-cell synapse is a function of RP (V):

$$I_{Ca}(t) = G_{Ca}^{max} m_{I_{Ca}}^3(t)(V(t) - E_{Ca}), \tag{1}$$

where G_{Ca}^{max} is the maximum conductance with all the calcium channels open, $m_{I_{Ca}}$ is the proportion of open channels (modeled as a Boltzman function of the RP), and E_{Ca} is the reversal potential of calcium. Calcium ion concentration, $[Ca^{2+}](t)$, is a low-pass function of current, and determines the probability of release of neurotransmitter vesicles:

$$k(t) = \max(([Ca^{2+}]^3(t) - [Ca^{2+}]_{thr}^3)z, 0), \tag{2}$$

where $k(t)$ is the instantaneous release probability of a vesicle, $[Ca^{2+}]_{thr}$ is the threshold calcium concentration for vesicle release, and z is a scalar.

Sumner *et al.* described how the model AN fiber response depends on the choice of two parameters in the calcium stage. The continuous lines in Fig. 1 show how rate-intensity (RI) functions vary with G_{Ca}^{max}. A large value of G_{Ca}^{max} (~8 nS) will result in a fiber with HSR type characteristics, while a small value (~2–4 nS) produces a LSR fiber. The dotted lines in Fig. 1 show how the RI functions vary with $[Ca^{2+}]_{thr}$. This parameter affects primarily the low-intensity responses, and thus affects the spontaneous rate and threshold of the unit. It allows for a largely independent control of the spontaneous rate. Together these two parameters afford excellent control over the rate responses of the model.

Adaptation in the model is due to depletion of the neurotransmitter available for release. Transmitter cycles around three reservoirs: the immediate store (q), where transmitter is ready for release; the synaptic cleft (c); and the reprocessing store (w), where transmitter is transported back in to the cell. This movement is modeled by three differential equations:

$$\frac{dq(t)}{dt} = N(w(t),x) + N([M - q(t)],y) - N(q(t),k(t)), \tag{3}$$

$$\frac{dc(t)}{dt} = N(q(t),k(t)) - lc(t) - rc(t), \tag{4}$$

$$\frac{dw(t)}{dt} = rc(t) - N(w(t),x); \tag{5}$$

x and r determine the rates of recycling. In addition, some transmitter is lost in the cleft (at a rate lc) and new transmitter is manufactured [at a rate proportional to $y(M-q)$]. Movement within the cell is a quantal stochastic process. $N(n,\rho)$ is a random process describing probabilistic transport of transmitter quanta. Each of n possible events has an equal probability, ρdt, of occurring in a single simulation epoch.

The model used here has been tuned to guinea-pig AN rate responses at a best frequency (BF) of 16.7 kHz. The complete set of parameter values is given in ''HSR set'' Table II, and ''AN set'' of Table III, of Sumner *et al.* The values of the parameters that are varied in this study are given in Table I.

III. MODELING AN ADAPTATION CHARACTERISTICS

A. Adaptation of HSR fibers

Westerman and Smith (Westerman, 1985; Westerman and Smith, 1984) have made extensive measurements of adaptation characteristics of gerbil AN fibers. These are thought to be very similar to the guinea-pig (Smith, 1977; Rhode and Smith, 1985). Adaptation can be described as a sum of two exponential functions fitted to a PSTH with a 1-ms bin-width:

$$R(t) = A_r e^{-t/t_r} + A_{st} e^{-t/t_{st}} + A_{ss}, \tag{6}$$

where A_r and A_{st} are the components of rapid and short-term adaptation, and A_{ss} is a steady-state component, while t_r and t_{st} are the respective decay time constants for the adaptation. Figure 2 compares model and gerbil data (Westerman, 1985) for all five components as a function of signal level. Since most AN fibers are of the HSR type, we compare the data with the HSR model of Sumner *et al.* (see Sec. II above). The unique parameters of this fiber are given in Table I. Figure 2(a) shows the two time constants of adaptation, t_r and t_{st}, as a function of stimulus level. The short-term time constant is stable between 10 and 40 dB SPL for both animal and the model while the rapid time constant falls over the same range for both. Figure 2(b) shows the components of rapid, short-term adaptation, and steady-state firing. The rapid component (A_r) is the largest, which has a larger dynamic range than the steady-state response (A_{ss}) for both the animal and model observations. The gray regions in the fig

TABLE I. Model parameters and summary results.

		HSR[a,b]	L3G[b]	H3E[b]	MSR[a]	L1[a]	L3C[b]
G_{Ca}^{max} (nS)		8	8	11	4.5	2.75	3.25
$[Ca^{2+}]_{thr}$ ($\times 10^{-11}$), Calcium conc.		4.48	5	5	3.2	4	4.48
M		10	10	10	10	8	10
Driven-recovery	(i) as a single exponential				√		
	(ii) faster for onset than steady state	√	√	√	√	x	x
Increments	(i) onset is additive	x	x	x	x	√	√
	(ii) short-term is additive				√		
Decrements	(i) onset is not additive	√	√	√	√	x	x
	(ii) short-term is additive	x	x	√	√	√	√
Conservation	(i) Rapid components				√		
	(ii) short-term components				√		
SR recovery	Fitted by a single exponential	√		√			

[a]Parameter sets used in Sumner *et al.* (2002).
[b]Parameter sets for fibers shown in Fig. 3. Except for HSR, first letter denotes SR, last denotes panel in Fig. 3 in which they appear.

ure represent the spread of estimates found by Westerman. The model results sit comfortably within those regions. The large steady-state response reflects the AN data to which the rate responses of the model were tuned in Sumner *et al.*

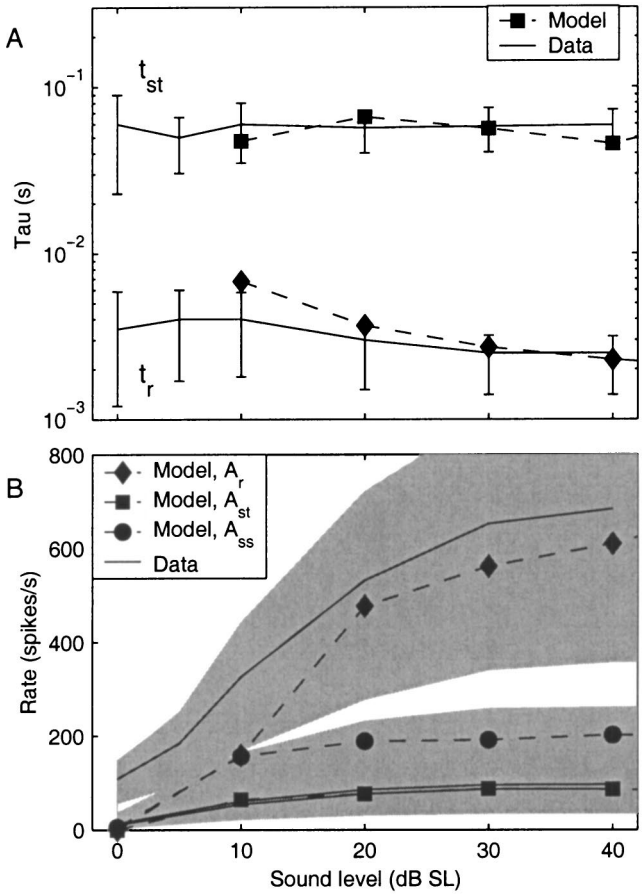

FIG. 2. AN adaptation characteristics. Continuous lines indicate the average values found by Westerman (1985). Connected symbols show the calculated coefficients of the model using the "AN set" DRNL parameters (Table III) and "HSR" synapse parameters (Table II) of Sumner *et al.*. The unique parameters of this model are also given here in Table I. (a) Rapid and short-term time constants of adaptation, t_r and t_{st}. Vertical bars show the standard deviation of the data. (b) Coefficients for rapid (A_r), short-term (A_{st}), and steady-state (A_{ss}) components of the response. Shaded areas show the range of values found by Westerman.

B. Variations in adaptation with fiber type

Rhode and Smith (1985) and Müller and Robertson (1991) investigated the variation in adaptation rates with fiber type, in cat and guinea-pig respectively. They found that HSR fibers show substantial adaptation with time while LSR fibers do not. Figures 3(a)–(d) compare the PSTH responses of two model fibers with guinea-pig data from Müller and Robertson (1991) for both HSR and LSR fibers. The difference in fiber type was modeled with only a reduction in G_{Ca}^{max}. The HSR model was the same as in Fig. 2, and the LSR model had $G_{Ca}^{max}=3.25$ nS. This model fiber will be referred to as L3C hereafter [it has a *Low* spontaneous rate and appears in Fig. 3(c)] and its unique parameters are listed in Table I. The resulting models reproduce qualitatively the observed difference in adaptation. In these simulations the synapse was fully recovered for each stimulus presentation. The lower rate of calcium influx of the LSR fiber means the synapse is driven less hard. As a consequence, transmitter depletion is not so rapid and adaptation is less marked. Both example data fibers show some adaptation at low levels. We were not able to reproduce this effect quantitatively in the model at these low firing rates by changing G_{Ca}^{max}.

Relkin and Doucet (1991) have found that LSR fibers in the chinchilla actually showed larger onsets than HSR fibers at long interstimulus intervals (>1 s). Their data suggest that LSR fibers take longer to recover from adaptation than HSR fibers and that the small amount of adaptation observed for LSR fibers in other studies was a result of a short (80 ms for Müller and Robertson) interstimulus interval. In Figs. 3(e)–(h) we consider PSTHs for fully recovered fibers, from Relkin and Doucet (1991). Figures 3(f) and (h) show two PSTHs in response to 100-ms tone bursts for a HSR and LSR fiber, respectively. Figure 3(e) illustrates the response of a HSR model fiber (H3E) that shows a response similar to the data. Figure 3(g) shows a LSR model (L3G). G_{Ca}^{max} is 8 nS for the L3G model and 11 nS for the H3E model. $[Ca^{2+}]_{thr}$ is 5×10^{-11} in both cases. This is slightly larger than the value of 4.48×10^{-11} used in the fibers HSR and L3C. The patterns of behavior seen in Fig. 3 arise from differences in the resting value of q, the number of vesicles in the immediate store.

Model compared with Müller and Robertson (1991).

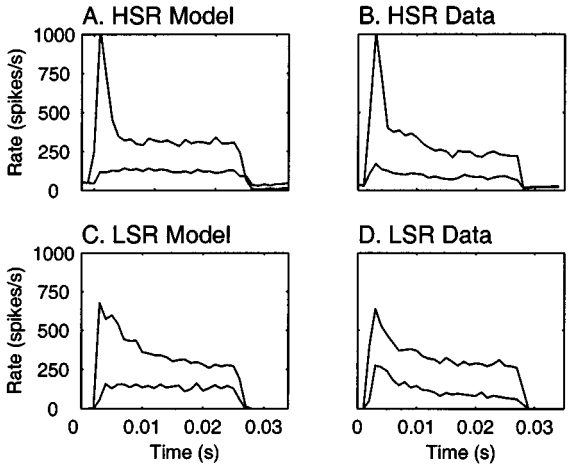

Model compared with Relkin and Doucet (1991).

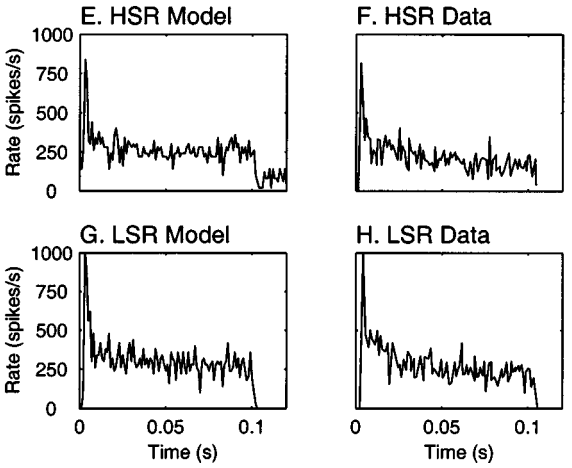

FIG. 3. The PSTH responses for tone bursts for HSR and LSR fibers, showing the variation in adaptation characteristics between fiber type and level. (a) Model response for 25-ms tone bursts at 10 kHz, 66 and 85 dB SPL, using the "AN set" DRNL (Table III) and "HSR" synapse (Table II) parameters of Sumner *et al.* (2002). Unique parameters are shown as "HSR" set in Table I here. (b) Guinea-pig HSR fiber with BF of 17 kHz for stimuli of (a). (c) Model fiber, with parameters as in (a) except $G_{Ca}^{max}=3.25$ nS, showing LSR type adaptation (L3C in Table I). Stimuli are at 12 kHz, 80 and 90 dB SPL. (d) Guinea-pig LSR fiber (from Müller and Robertson, 1991) with a BF of 20.5 kHz for the same stimuli as (c). (e) Model showing HSR response to a 100-ms tone. Parameters as in (a) except $G_{Ca}^{max}=11$ nS, and $[Ca^{2+}]_{thr}=5\times10^{-11}$ (H3E in Table I). (f) Chinchilla HSR fiber. (g) Model showing LSR response. Parameters as in (a) except $G_{Ca}^{max}=8$ nS, and $[Ca^{2+}]_{thr}=5\times10^{-11}$ (L3G in Table I). (h) Chinchilla LSR fiber (from Relkin and Doucet, 1991). (e)–(h) all use BF tone pips at 40 dB above threshold.

The unadapted vesicle release rate is qk [see Eq. (3)]. The H3E model fiber has a resting value for q of approximately 6. This is smaller than the maximum value (M) because of frequent spontaneous releases. The L3G model fiber has no spontaneous rate, and consequently $q=M=10$ in the absence of stimulation. The difference in q is larger than the opposing difference in k. Therefore, the L3G model has the stronger onset response. This mechanism is similar to the speculations of Relkin and Doucet.

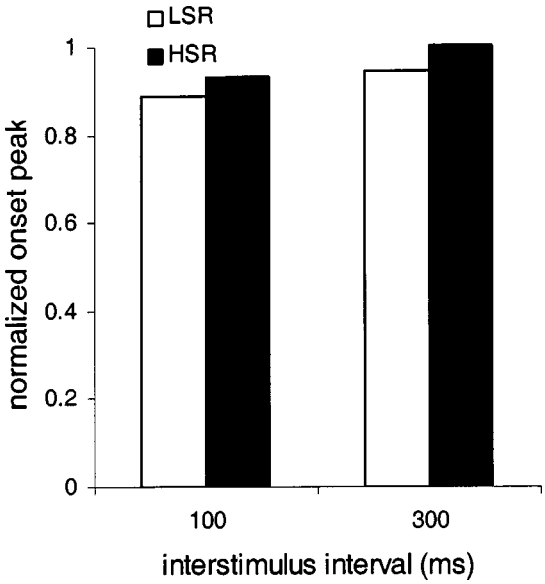

FIG. 4. Effect of interstimulus interval on normalized onset rates for two model fibers. The solid bars show the response of the HSR model fiber and the open bars show the response of the L1 fiber. The onset-rate is normalized by the onset peak measured at an interstimulus-interval of two seconds.

Relkin and Doucet (1991) found that an interspike interval (ISI) of 300 ms was adequate to demonstrate complete recovery in HSR fibers. However, LSR fibers were only 80% recovered by that time. We have simulated their experiment 2 using the model fibers HSR and L1. The tone stimuli were 100 ms in duration and were presented repeatedly with a separation of either 100 or 300 ms for 600 trials. The dependent variable was the onset spike rate computed using the number of spikes in the most populated 1-ms bin of the PSTH after the onset of the stimulus. The onset rate was normalized relative to the fully recovered rate observed when the ISI was 2 s. The stimuli were presented at 50 and 80 dB SPL for fibers HSR and L1, respectively; 40 dB above threshold in both cases. The model results, which show the same effect as Relkin and Doucet, are shown in Fig. 4. The HSR fiber is almost completely recovered when the ISI is 300 ms but the LSR fiber is less than 90% recovered despite a higher rate of response at the 100-ms ISI.

IV. MODELING OTHER MEASURES OF AN ADAPTATION

There are many other measures of AN adaptation processes. Other studies (Hewitt and Meddis, 1991; Ross, 1996) have modeled a range of these measures. The model of Meddis (1986, 1988) was among the models tested there. Here we will test the revised version of the model for the same measures, in order to compare its performance with previous models. No attempt has been made to vary the parameters to optimize the fit of the revised model to these responses. Instead, we have used three model fibers that have already been presented in this study and three from Sumner *et al.* (2002). The unique parameters of the fibers are given in

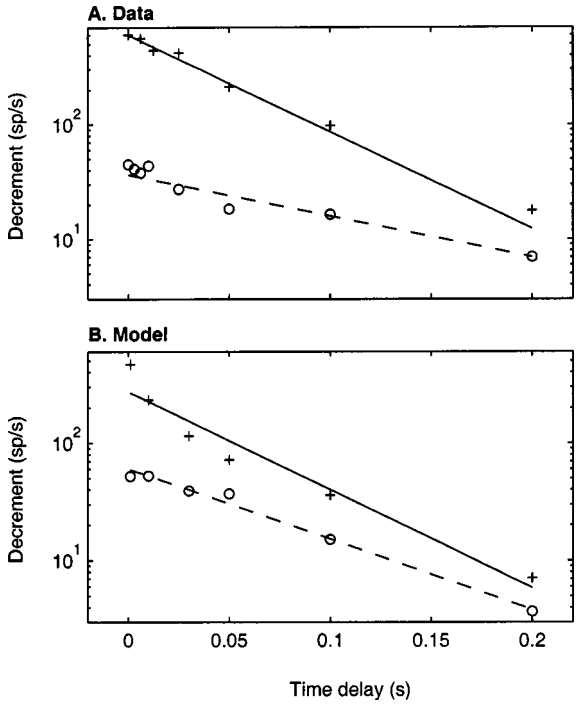

FIG. 5. Recovery of driven responses to sound. (a) Data from Westerman (1985): the decrement in firing rate of the onset (1-ms window at probe onset; crosses are data and continuous line is the fitted recovery function) and short-term (last 20 ms of probe; circles are data and dashed line is the fitted recovery function) portions of the response to a 43 dB SL 30-ms tone, when preceded by a 300-ms masker at the same level. (b) Averaged responses of model fibers HSR, MSR, H3E, and L3G for the paradigm of Westerman.

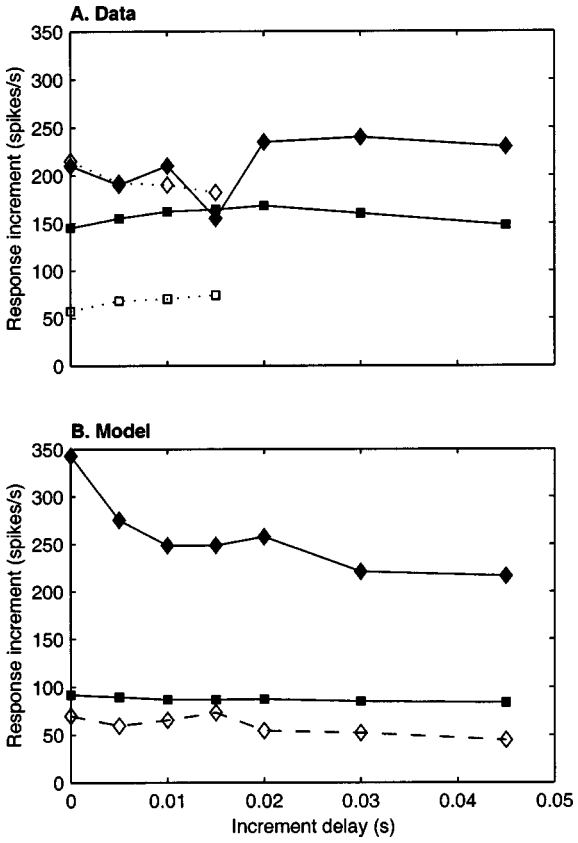

FIG. 6. Increments in firing rate in response to increments in stimulus level. (a) Data from Smith *et al.* (1985) showing the increment in firing rate with onset (continuous lines and filled diamonds) and short-term (continuous lines and filled squares) window analyses, for different increment delays. The stimulus is a 60-ms BF tone, which starts at 13 dB SL and subsequently increases in level by 6 dB. Also shown are the results of Winter *et al.* (1993) as dashed lines and open symbols (diamonds are onset window increments and squares are short-term window increments). (b) Results of applying the paradigm of Smith *et al.* to the model fibers: (diamonds and continuous line), average onset-window increments for fibers: HSR, MSR, H3E, and L3G; (open diamonds and dashed line), average of onset responses for remaining model fibers (L1 and L3C); (filled squares and continuos line), average of short-term window responses for all fibers.

Table I. All other parameters are the same as the ''AN set'' DRNL parameters (Table III) and ''HSR'' synapse parameters (Table II) of Sumner *et al.*

A. Recovery of responses to stimulation

The response of AN fibers to acoustic simulation is reduced immediately following prior stimulation. This is presumed to be a function of the adaptation observed during stimulation, and is probably in part responsible for the psycho-acoustical phenomenon of forward masking (Moore, 1997). Forward-masking paradigms have been used to study the recovery of AN responses (e.g., Smith, 1977; Harris and Dallos, 1979; Westerman, 1985). Figure 5(a) shows an example of the response of a gerbil AN fiber from Westerman. He used a 300-ms ''masker'' followed by a 30-ms probe at various delays. He analyzed the response of the probe for 1-ms windows at the onset of the probe response (onset window) and windows covering the last 20 ms of the response (short-term window) in order to reveal the recovery of rapid and short-term adaptation processes. The upper data set (crosses and continuous fitted line) is the onset window response, expressed as a decrement in firing rate relative to the corresponding portion of the masker. The lower data set (open circles and dashed fitted line) is the short-term window decrement. Westerman found, in 11 fibers, that the onset response recovered with a mean time constant of 50 ms, and the short-term window response recovered with a mean time constant of about 170 ms. Figure 5(b) shows the average of the responses of the model fibers HSR, MSR, H3E, and L3G. The responses show a good resemblance to the data, including slightly differing time constants for fast and slow recovery. The difference is attributable to the large onset-window decrements at delays of less than 5 ms that increase the gradient of the best-fit line.

B. Increments

Smith and Zwislocki (1975), in the gerbil, found that the increase in firing rate in response to an increment in stimulus level does not greatly depend on the time between the onset of the tone and the subsequent increment in level. This suggested that adaptation was additive. Smith *et al.* (1985) found that this also held if increments were analyzed with window lengths that separated rapid and short-term adaptation. Figure 6(a) shows the results of Smith *et al.* The stimulus used was a 60-ms BF pedestal tone, at 13 dB SL, with a 6-dB increase in level occurring at various delays up to 40 ms after the start of the pedestal. The diamonds joined by continuous lines indicate the response analyzed over a 1-ms window (onset window) at the start of the response to the

increment. The squares joined by continuous lines show the response over a 10-ms window (short-term window) starting at the same time as the onset window. Smith's results are additive in the sense that the effect of an increment in stimulus intensity is the same irrespective of the time at which the increment is introduced.

Winter *et al.* (1993), using guinea-pigs, subsequently found that onset increments show a statistically significant increase at delays of less than 5 ms. The effect of all other increments were additive. These results are also shown in Fig. 6(a) (open symbols and dashed lines). Westerman's average data also show slight departure from additivity for onset-window increments at short delays. The ratio of the increments at a delay of 0 ms to a delay of 30 ms was 1.2.

Figure 6(b) shows the results of simulating the increment paradigm of Smith *et al.* for the six model fibers. The squares joined by continuous lines show the short-term window increment averaged over all six model fibers. The results show additivity throughout except for increased responses at short delays for onset windows. This agrees quite well with the average measurements of Winter *et al.* (1993). The diamonds joined by a continuous-line show the average of the onset window increments for three model fibers (HSR, H3E, L3G). These fibers all displayed departure from additivity at short delays. The ratio of the increments at $t=0$ to $t=30$ ms is 1.44. This trend is the same as found by Winter *et al.*, although the departure from additivity is greater in the model. The open diamonds joined with a dashed line show the average of the onset-window increment for the three remaining model fibers (MSR, L1, L3C). They were additive for all delays in agreement with Smith's data. This line falls below that of the average short-term response, because the firing rates of fibers L1 and L3C are considerably less than the other fibers.

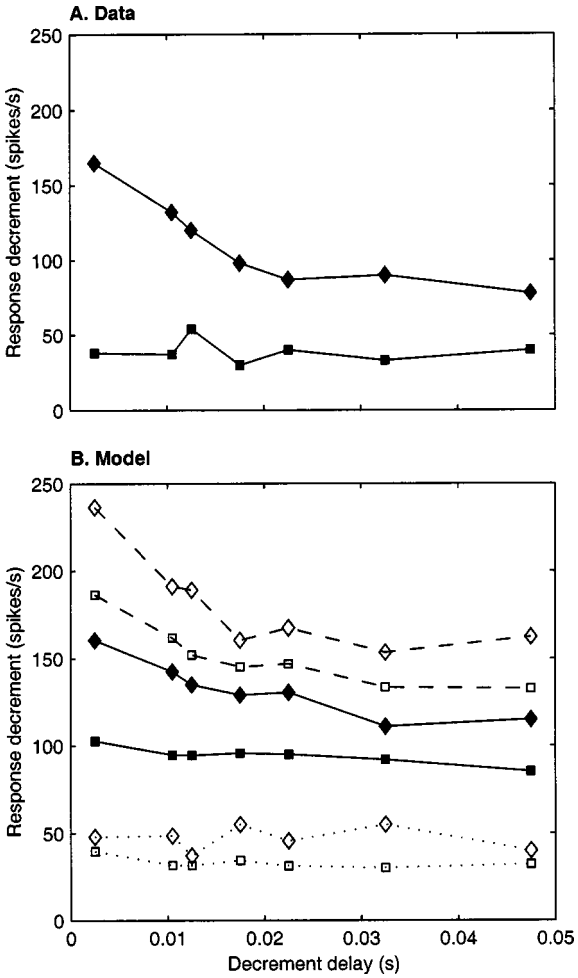

FIG. 7. Decrements in firing rate in response to decrements in stimulus level. (a) Data from Smith *et al.* (1985) showing the decrement in firing rate of onset-window (diamonds) and short-term window (squares) analyses for different decrement delays. The stimulus is a 60-ms BF tone, which starts at 13 dB SL and subsequently drops in level by 6 dB. (b) Results of applying the paradigm of Smith *et al.* to the model fibers. Diamonds show onset-window decrements and squares are short-term window decrements: continuous lines with filled symbols are fibers MSR and H3E; dashed lines with open symbols are fibers HSR and L3G; dotted lines with open symbols are L1 and L3C.

C. Decrements

The change in AN firing rates has also been studied for decrements in stimulus level. Decrement responses were found to be additive for short-term window analysis, but onset window decrements were clearly not additive. Figure 7(a) shows an example of the response of a gerbil AN fiber to decrements (Smith *et al.*, 1985). The stimulus was a 60-ms BF tone, which started at a level of 13 dB SL, and dropped by 6 dB after various intervals. The analysis windows were of the same form as used for measuring increments. The short-term window decrement (continuous line and squares) remains roughly constant with decrement delay. In contrast, the onset-window decrement (continuous line and diamonds) depends strongly on the decrement delay. Smith found this result to hold in nine units. The average ratio of the decrements at 30 to 0 ms was 0.56 for the onset-window decrement and 0.93 for the short-term-window decrement. Figure 7(b) shows the response of the six model fibers to the same paradigm. Squares indicate short-term decrements and diamonds denote onset decrements. The closest result to the data is for the MSR and H3E fiber models averaged together (continuous lines and filled symbols). Both onset and short-term components qualitatively resemble the data, although the departure from additivity for the onset response was not very marked. The model fibers HSR and L3G also gave very similar results and have been averaged together (dashed lines and open symbols). They showed realistic onsets, but did not show additivity for the short-term window analysis. The two LSR remaining fibers (L1, L3C) were also very similar and are shown averaged (dotted lines and open symbols). These showed additivity in both short-term and onset responses. The model is clearly capable of a diverse range of responses, some agreeing well with the data. Averaging the ratios of decrements at 30 to 0 ms for the model fibers HSR, L3G, MSR, and H3E yields 0.69 for the onset response and 0.79 for the short-term responses. L1 and L3C were excluded to make the sample more representative of Westerman's data.

D. Conservation

Westerman (1985; Westerman and Smith, 1987) characterized the transient AN responses for two contiguous 300-ms tone bursts, with the first tone varying in level, and

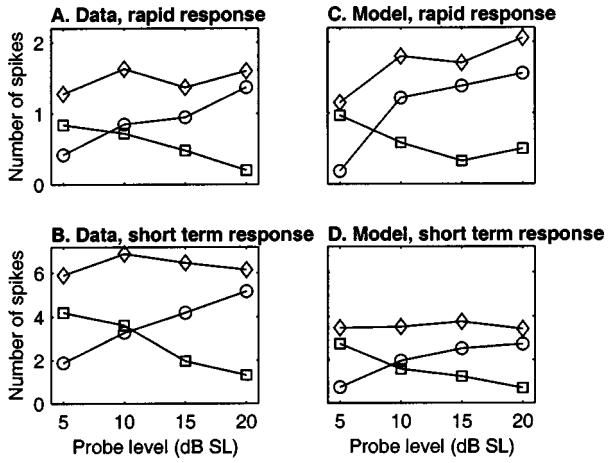

FIG. 8. Conservation of AN adaptation. (a) and (b) the rapid and short-term components averaged across seven gerbil fibers, from Westerman and Smith (1987). A 300-ms background tone of varying sensation level is followed by a contiguous 300-ms increment, fixed at 43 dB SL. Squares show the response of the increment period. Circles show the response during the background time. Diamonds show the total of both background and increment. (c) The average rapid components responses of the four model fibers HSR, MSR, H3E, and L3G. (d) The average short-term components of all the model fibers.

the second tone fixed at a higher level. He found that as the level of the first tone increased, the amount of transient response associated with it also increased. At the same time the transient activity in the second tone decreased. The combined transient response associated with the two tones remained roughly constant. He termed this property ''conservation.'' Figures 8(a) and (b) show the average results of seven gerbil fibers reported by Westerman and Smith. A 43 dB SL tone is preceded by a tone at four different levels (5, 10, 15, or 20 dB SL). The transient responses are characterized by fitting Eq. (6) to each portion of the response separately. The total amount of transient activity associated with rapid and short-term adaptation is then described by $A_r\tau_r$ and $A_{st}\tau_{st}$, respectively. Figure 8(c) shows the number of spikes associated with the rapid component, averaged across the four of the model fibers HSR, MSR, H3E, and L3G. The LSR model fibers L1 and L3C were omitted because they did not show any significant rapid component. The total rapid activity does show some increase with level. Figure 8(d) shows the spikes associated with the short-term component, averaged across all six model fibers. This shows excellent conservation of the total short-term adaptation, although the absolute number of spikes associated with the transient components is lower than the data.

E. Recovery of spontaneous activity

Immediately after the onset of a tone, spontaneous activity of AN fibers is greatly reduced for several tens of milliseconds. The recovery of spontaneous firing can be described by a single exponential function. A range of time constants have been described for different species from 20 to 100 ms, depending on stimulus level (Smith, 1977; Harris and Dallos, 1979; Westerman, 1985). We fitted exponential functions to the recovery of spontaneous activity for the model fibers HSR and H3E. The models were stimulated for 100 ms at 40 dB SPL, as in Hewitt and Meddis (1991). The time constants were 25 ms for the HSR model, and 22 ms for the H3E model. Hewitt and Meddis (1991) reported 30 ms for the original Meddis model. These values are in good agreement with the average value of 20 ms measured by Yates *et al.* (1985) for the guinea-pig, although they are on the low end of the range of values reported across other studies.

V. INNER WORKINGS OF THE MODEL

This section illustrates the operation of the model for two simple cases. The vibration of the basilar membrane gives rise to RP changes that lead to calcium flow into the cell. It is the accumulation of calcium that controls the release of vesicles of transmitter into the synaptic cleft. Both the half-wave rectified RP and the calcium accumulation are subject to low-pass filtering. As a result, constant-intensity, high-frequency tones produce a steady dc response. This is a useful simplification when studying the response at the synapse. We can think of the proximal stimulus at the synapse as a step function at the onset and offset of the stimulus.

Figure 9(a) shows the transmitter flow arrangements. Calcium accumulates in the cell at a rate determined by the RP. This accumulation causes transmitter to be released from the available pool (q) into the synaptic cleft (c). In the cleft, the transmitter has postsynaptic effects and some of it is lost but most is taken back into the cell where it is stored in a reprocessing pool (w). From there it is eventually returned to the available pool. Losses from the cleft are replaced by manufacture of new transmitter.

Figure 9(b) shows the changes in the values of q, c, and w when a high-frequency tone is presented only once against a background of silence. A high-intensity (90 dB SPL) tone and a LSR fiber (L3G) are chosen for clearest presentation. Following tone onset, the transmitter in the available store, q, is reduced and pulses of transmitter can be seen in the synaptic cleft, c, as individual vesicles are released. Very soon, the transmitter in the reprocessing store, w, has increased as the transmitter is recycled back from the cleft. Following tone offset, q recovers partly as the result of input from the reprocessing store and partly from replenishment through manufacture of new transmitter. Toward the end of the tone, there is enough transmitter in the reprocessing store to make four replacement vesicles. However, the available pool must recover from almost zero to ten vesicles. The balance comes from remanufacture at a much slower rate. In our example, the final replacement vesicle does not arrive until 100 ms after the end of the stimulus. The rate of manufacture is given by the expression, $y(M-q)$. As q increases during recovery, this rate becomes smaller.

Figure 9(c) shows a different pattern of response. The stimulating tone is now only 50 dB SPL and the fiber is HSR. Release into the cleft is continuous, even during silence. The resting level of q, the available store, is variable but typically below the maximum, M, of 10. This is an important consideration because ''recovery'' is complete for HSR model fibers when this resting level is reached, not when the maximum level is reached, as was the case for the L3G fiber. The available store does not become fully depleted at this level of

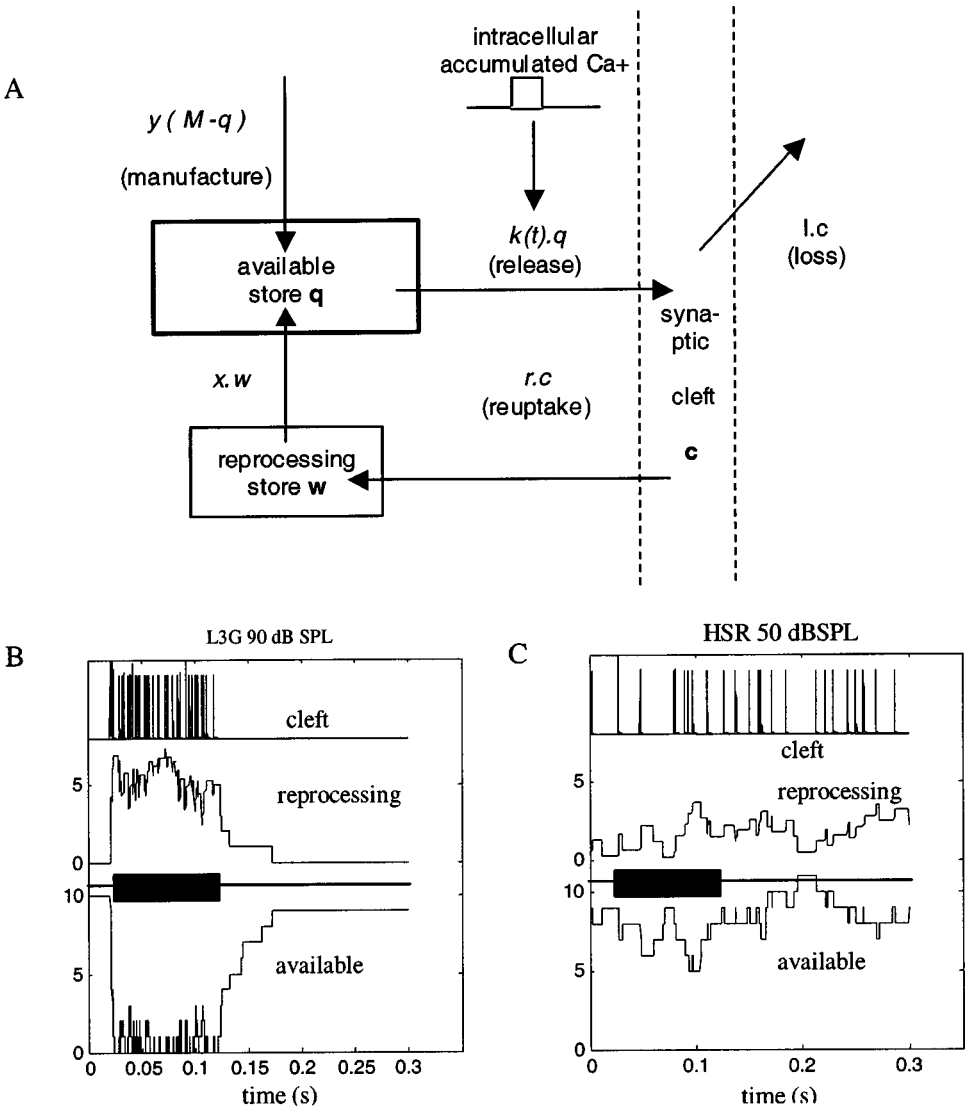

FIG. 9. The inner workings of the model. (a) Schematic of the recycling of neurotransmitter around the internal reservoirs. (b) The contents of the presynaptic reservoirs of the L3G fiber in response to a 100-ms tone burst at 90 dB SPL. (c) The contents of the presynaptic reservoirs of the HSR fiber in response to a 100-ms tone burst at 50 dB SPL. The reservoirs, arranged from top to bottom, are the cleft (c), reprocessing (w), and the immediately available store (q). The black bar shows the presence of the stimulating tone.

stimulation. It shows only a gentle depression after the tone onset. Under these conditions, recovery of the transmitter levels in the available store is mostly sourced from the reprocessing store. Thus differences in adaptation behavior arise from changes in the input to the adaptation mechanism alone.

VI. DISCUSSION

The basic adaptation characteristics of the revised model fall well within the range described by Westerman for the gerbil. The modifications required to make the new model included additional low-pass filtering, quantal stochastic vesicle release, and refractory effects. These changes did not greatly affect the characteristics of adaptation HSR model, and the parameter values for the synapse have changed little from Meddis *et al.* (1990).

Rhode and Smith (1985) and Müller and Robertson (1991) found that LSR fibers show very little adaptation. The data of Relkin and Doucet (1991) suggests that the lack of adaptation observed was due to an insufficient time for recovery between stimuli, and that fully recovered LSR fibers actually show more adaptation than HSR fibers. The model can reproduce the data of Müller and Robertson and Relkin and Doucet even when the simulations are fully recovered for each stimulus presentation. In addition the model can also be affected by interstimulus interval. Although highly speculative, the flexibility of the model raises the possibility that interstimulus intervals might not explain all the differences between observation. It is interesting to note that the three studies all used different species, and different divisions of spontaneous-rate classes. Species differences seem to exist for RI functions. Purely straight RI functions have been associated with LSR fibers in guinea-pig (Winter *et al.*, 1993). We know of no data showing such functions in other species. The different LSR model fibers have quite different RI functions. The L3C model used to model guinea-pig PSTH has a straight, sloping shape, while the L3G fiber's RI function is steep (see Fig. 1). More data may clarify how to set up the model.

The differences in adaptation with fiber type in the model extend to measures of recovery, and stimulus increments and decrements. Overall, the model is not additive enough. However, average data suggests that the issue is not completely clear-cut, and the lack of additivity in the model is not as great as presented previously (Hewitt and Meddis, 1991). The different model fibers show different patterns of

response, and the LSR model fibers especially differ from the responses reported previously. Unfortunately, the data modeled cannot inform us of variation of these characteristics with fiber class, as they are of small numbers of fibers, and naturally biased towards higher spontaneous rates.

It is interesting that the model parameters determining rate characteristics also affect the adaptation characteristics, without any change to the adaptation mechanism itself. Differences in adaptation occur when the driving force to the synapse, or the resting supply of vesicles, varies. Changes in adaptation are to be expected if the difference between fiber types is located before the adaptation mechanism. Thus differences in adaptation between fiber types may offer clues to the location of fiber difference.

ACKNOWLEDGMENTS

This research was supported by the Wellcome foundation (grant ref. 003227), and also by the Consejería de Sanidad of the Junta de Comunidades de Castilla-La Mancha (ref. 01044). The authors would like to thank the two anonymous reviewers for their efforts, and to acknowledge Evan Relkin for his valuable input on the material that was originally submitted as part of Sumner *et al.* (2002).

Harris, D. M., and Dallos, P. (**1979**). ''Forward masking of auditory nerve fiber responses,'' J. Neurophysiol. **42**, 1083–1106.

Hewitt, M., and Meddis, R. (**1991**). ''An evaluation of eight computer models of mammalian inner hair-cell function,'' J. Acoust. Soc. Am. **90**, 904–917.

Meddis, R. (**1986**). ''Simulation of mechanical to neural transduction in the auditory receptor,'' J. Acoust. Soc. Am. **79**, 702–711.

Meddis, R. (**1988**). ''Simulation of auditory-neural transduction: Further studies,'' J. Acoust. Soc. Am. **83**, 1056–1063.

Meddis, R., Hewitt, M., and Shackleton, T. (**1990**). ''Implementation details of a computational model of the inner hair-cell/auditory-auditory nerve synapse,'' J. Acoust. Soc. Am. **87**, 1813–1816.

Müller, M., and Robertson, D. (**1991**). ''Relationship between tone burst discharge pattern and spontaneous firing rate of auditory nerve fibers in the guinea-pig,'' Hear. Res. **57**, 63–70.

Moore, B. C. J. (**1997**). *An Introduction to the Psychology of Hearing* (Academic, New York), 4th ed.

Relkin, E. M., and Doucet, J. R. (**1991**). ''Recovery from prior simulation I: Relationship to spontaneous firing rates of primary auditory neurons,'' Hear. Res. **55**, 215–222.

Rhode, W. S., and Smith, P. H. (**1985**). ''Characteristics of tone-pip response patterns in relationship to spontaneous rate in cat auditory nerve fibers,'' Hear. Res. **18**, 159–168.

Ross, S. (**1996**). ''A functional model of the hair-cell primary fiber complex,'' J. Acoust. Soc. Am. **99**, 2221–2238.

Shamma, S. A., Chadwick, R. S., Wilbur, W. J., Morrish, K. A., and Rinzel, J. (**1986**). ''A biophysical model of the cochlear processing: Intensity dependence of pure tone responses,'' J. Acoust. Soc. Am. **80**, 133–145.

Smith, R. L. (**1977**). ''Short-Term Adaptation in Auditory-Nerve Fibers: Some poststimulatory effects,'' J. Neurophysiol. **40**, 1098–1112.

Smith, R. L., and Zwisloki, J. J. (**1975**). ''Short-term adaptation and incremental responses of single auditory-nerve fibers,'' Biol. Cybern. **17**, 169–182.

Smith, R. L., Brachman, M. L., and Frisina, R. D. (**1985**). ''Sensitivity of auditory nerve fibers to changes in intensity: A cichotomy between decrements and increments,'' J. Acoust. Soc. Am. **78**, 1310–1316.

Sumner, C. J., Lopez-Poveda, E. A., O'Mard, L. P., and Meddis, R. (**2002**). ''A revised model of the inner-hair cell and auditory nerve complex,'' J. Acoust. Soc. Am. **111**, 2178–2188.

Westerman, L. A. (**1985**). ''Adaptation and recovery of auditory nerve responses,'' Special report ISR-S-24, Syracuse University.

Westerman, L. A., and Smith, R. L. (**1984**). ''Rapid and short-term adaptation in auditory nerve responses,'' Hear. Res. **15**, 249–260.

Westerman, L. A., and Smith, R. L. (**1987**). ''Concervation of adapting components in auditory nerve responses,'' J. Acoust. Soc. Am. **81**, 680–691.

Westerman, L. A., and Smith, R. L. (**1988**). ''A diffusion model of the transient response of the cochlear inner hair cell synapse,'' J. Acoust. Soc. Am. **83**, 2266–2276.

Winter, I. M., Palmer, A. R., and Meddis, R. (**1993**). ''The response of guinea-pig auditory nerve fibers with high-spontaneous discharge rates to increments in intensity,'' Brain Res. **618**, 167–170.

Yates, G. K., Robertson, D., and Johnstone, B. M. (**1985**). ''Very rapid adaptation in the guinea-pig auditory nerve,'' Hear. Res. **17**, 1–12.